Eur J Nucl Med Mol Imaging (2012) 39:512–520
DOI 10.1007/s00259-011-2008-5

ORIGINAL ARTICLE

Biodistribution, radiation dosimetry and scouting of ^{90}Y-ibritumomab tiuxetan therapy in patients with relapsed B-cell non-Hodgkin's lymphoma using ^{89}Zr-ibritumomab tiuxetan and PET

Saiyada N. F. Rizvi · Otto J. Visser · Maria J. W. D. Vosjan · Arthur van Lingen · Otto S. Hoekstra · Josée M. Zijlstra · Peter C. Huijgens · Guus A. M. S. van Dongen · Mark Lubberink

Received: 12 August 2011 / Accepted: 15 November 2011 / Published online: 5 January 2012

Abstract
Purpose Positron emission tomography (PET) with ^{89}Zr-ibritumomab tiuxetan can be used to monitor biodistribution of ^{90}Y-ibritumomab tiuxetan as shown in mice. The aim of this study was to assess biodistribution and radiation dosimetry of ^{90}Y-ibritumomab tiuxetan in humans on the basis of ^{89}Zr-ibritumomab tiuxetan imaging, to evaluate whether co-injection of a therapeutic amount of ^{90}Y-ibritumomab tiuxetan influences biodistribution of ^{89}Zr-ibritumomab tiuxetan and whether pre-therapy scout scans with ^{89}Zr-ibritumomab tiuxetan can be used to predict biodistribution of ^{90}Y-ibritumomab tiuxetan and the dose-limiting organ during therapy.
Methods Seven patients with relapsed B-cell non-Hodgkin's lymphoma scheduled for autologous stem cell transplantation underwent PET scans at 1, 72 and 144 h after injection of ~70 MBq ^{89}Zr-ibritumomab tiuxetan and again 2 weeks later after co-injection of 15 MBq/kg or 30 MBq/kg ^{90}Y-ibritumomab tiuxetan. Volumes of interest were drawn over liver, kidneys, lungs, spleen and tumours. Ibritumomab tiuxetan organ absorbed doses were calculated using OLINDA. Red marrow dosimetry was based on blood samples. Absorbed doses to tumours were calculated using exponential fits to the measured data.
Results The highest ^{90}Y absorbed dose was observed in liver (3.2±1.8 mGy/MBq) and spleen (2.9±0.7 mGy/MBq) followed by kidneys and lungs. The red marrow dose was 0.52±0.04 mGy/MBq, and the effective dose was 0.87±0.14 mSv/MBq. Tumour absorbed doses ranged from 8.6 to 28.6 mGy/MBq. Correlation between predicted pre-therapy and therapy organ absorbed doses as based on ^{89}Zr-ibritumomab tiuxetan images was high (Pearson correlation coefficient r=0.97). No significant difference between pre-therapy and therapy tumour absorbed doses was found, but correlation was lower (r=0.75).
Conclusion Biodistribution of ^{89}Zr-ibritumomab tiuxetan is not influenced by simultaneous therapy with ^{90}Y-ibritumomab tiuxetan, and ^{89}Zr-ibritumomab tiuxetan scout scans can thus be used to predict biodistribution and dose-limiting organ during therapy. Absorbed doses to spleen

Saiyada N.F. Rizvi and Otto J. Visser contributed equally to this work.

S. N. F. Rizvi (✉) · A. van Lingen · O. S. Hoekstra · M. Lubberink
Department of Nuclear Medicine and PET Research,
VU University Medical Center,
PO Box 7057, De Boelelaan 1117,
1007 MB Amsterdam, The Netherlands
e-mail: snf.rizvi@vumc.nl

O. J. Visser · J. M. Zijlstra · P. C. Huijgens
Department of Haematology, VU University Medical Center,
De Boelelaan 1117,
1007 MB Amsterdam, The Netherlands

M. J. W. D. Vosjan · G. A. M. S. van Dongen
Department of Otolaryngology and Head and Neck Surgery,
VU University Medical Center,
De Boelelaan 1117,
1007 MB Amsterdam, The Netherlands

M. Lubberink
Department of Nuclear Medicine & PET, Uppsala University,
and Medical Physics, Uppsala University Hospital,
751 85 Uppsala, Sweden

were lower than those previously estimated using ^{111}In-ibritumomab tiuxetan. The dose-limiting organ in patients undergoing stem cell transplantation is the liver.

Keywords Immuno-PET · Molecular imaging · Radioimmunotherapy · Ibritumomab tiuxetan · ^{89}Zr · ^{90}Y · Dosimetry · Lymphoma

Introduction

Non-Hodgkin's lymphomas (NHL) account for 3% of all cancers worldwide [1]. Not all patients are cured with standard induction treatment [2]. For patients with aggressive, relapsed or progressive disease after first-line (immuno-) chemotherapy, a second-line regimen consisting of reinduction chemotherapy and consolidation with high-dose chemotherapy (carmustine, etoposide, cytarabine, melphalan; BEAM) followed by autologous stem cell transplantation (auSCT) is standard therapy with curative intent. A significant number of these patients will not be able to meet response criteria before transplantation or will relapse after transplantation [3]. The addition of anti-CD20 monoclonal antibodies (mAb) has substantially improved response rates and overall survival [4–6]. The ^{90}Y-labelled anti-CD20 mAb ibritumomab tiuxetan (Zevalin®) is approved for treatment of patients with relapsed and refractory NHL. In recent studies, radioimmunotherapy (RIT) was integrated into upfront treatment in indolent NHL [7] or added to high-dose chemotherapy followed by auSCT, showing significant benefit [8, 9]. In standard treatment, the maximum amount of ^{90}Y-ibritumomab tiuxetan given to patients is 15 MBq/kg with a maximum of 1.2 GBq [10]. The dose-limiting toxicity of RIT is myelosuppression. The effect of myelosuppression is prevented in auSCT with stem cell support. In general, higher external radiation doses are associated with improved clinical outcomes [11, 12]. To optimize therapeutic amounts of activity in individual patients, one needs to know the biodistribution of ^{90}Y-ibritumomab tiuxetan and the effective dose to dose-limiting organs.

Biodistribution studies with ^{111}In-ibritumomab tiuxetan and ^{131}I-ibritumomab tiuxetan in humans have been published [e.g. 13, 14]. These studies were performed using gamma cameras, which complicates quantification. Labelling of ibritumomab tiuxetan with the positron-emitting isotope ^{89}Zr allows for better quantitative assessment of biodistribution of ibritumomab tiuxetan with positron emission tomography (PET). Perk et al. [15] used *N*-succinyl-desferal for coupling of ^{89}Zr to ibritumomab tiuxetan and showed that ^{89}Zr-ibritumomab tiuxetan has a nearly identical biodistribution compared with ^{90}Y-ibritumomab tiuxetan in mice, which allows for assessment of biodistribution of ^{90}Y-ibritumomab tiuxetan using ^{89}Zr-ibritumomab tiuxetan and PET. A scout scan procedure using ^{89}Zr-ibritumomab tiuxetan to assess biodistribution of ibritumomab tiuxetan prior to therapy can then aid in selection of patients that can benefit from a potentially toxic therapeutic amount of ^{90}Y-ibritumomab tiuxetan, as well as in optimizing the administered amount of ^{90}Y-ibritumomab tiuxetan in the individual patient. However, even though ^{89}Zr-ibritumomab tiuxetan is representative of ^{90}Y-ibritumomab tiuxetan, a scout scan procedure with ^{89}Zr-ibritumomab tiuxetan for this purpose is only valid when biodistribution during scout scan and therapy are similar, that is not dependent on the administered amount of labelled antibody.

The aim of this clinical, prospective study was to assess biodistribution and radiation dosimetry of ^{90}Y-ibritumomab tiuxetan in humans using ^{89}Zr-ibritumomab tiuxetan and to investigate whether pre-therapy scout scans with ^{89}Zr-ibritumomab tiuxetan can be used to predict biodistribution during therapy, that is whether a co-injection of a therapeutic amount of ^{90}Y-ibritumomab tiuxetan influences biodistribution of ^{89}Zr-ibritumomab tiuxetan. A secondary aim was to determine the dose-limiting organ for therapy with ^{90}Y-ibritumomab tiuxetan, in order to enable dose escalation and/or optimization with ^{90}Y-ibritumomab tiuxetan in patients undergoing auSCT.

Materials and methods

Patients

Seven patients with relapsed or refractory aggressive B-cell (CD20-positive) NHL, who did not qualify for standard auSCT and were younger than 66, were included. All patients had previously been treated in first line with R-CHOP (cyclophosphamide, doxorubicin hydrochloride, vincristine and prednisolone, combined with rituximab). Second-line chemotherapy consisted of R-DHAP (cisplatin, cytarabine, dexamethasone combined with rituximab), R-VIM (etoposide, ifosfamide, methotrexate, combined with rituximab) and R-DHAP, which did not lead to at least partial remission as monitored by ^{18}F-fluorodeoxyglucose (FDG) PET.

All patients had a WHO performance status of 0–2. Exclusion criteria were history of intolerance to exogenous protein administration, severe cardiac dysfunction [New York Heart Association (NYHA) functional classification class II–IV], severe pulmonary dysfunction (vital capacity or diffusion capacity<70%), unless clearly related to NHL involvement, hepatic dysfunction, bilirubin or transaminase≥2.5 times the upper normal limit, renal dysfunction (serum creatinine≥180 μmol/l or clearance≤40 ml/min), prior treatment with radiation therapy, uncontrolled infections, human immunodeficiency virus (HIV) positive and

NHL localization in the central nervous system. The study was approved by the Medical Ethics Committee of the VU University Medical Center and all patients signed a written informed consent prior to inclusion.

Synthesis of ^{89}Zr-ibritumomab tiuxetan and ^{90}Y-ibritumomab tiuxetan

Ibritumomab tiuxetan was obtained from Bayer Schering AG (Berlin, Germany). ^{90}Y (18.5 GBq/ml, radioactive half-life $T_{1/2}$=64.1 h) was obtained from IBA (Louvain-la-Neuve, Belgium) and ^{90}Y-ibritumomab tiuxetan was prepared according to instructions of the supplier. ^{89}Zr (≥0.15 GBq nmol^{-1}, $T_{1/2}$=78.5 h) was produced in-house by a (p,n) reaction on natural ^{89}Y and isolated with the use of a hydroxamate column [16]. Methods for radiolabelling were used as described previously [15]. ^{89}Zr-ibritumomab tiuxetan conjugates were analysed by instant thin-layer chromatography (ITLC) for radiochemical purity, and by a cell binding assay for immunoreactivity, as described before [16]. Endotoxin levels were assessed by use of a limulus amebocyte lysate (LAL) test system licensed by the US Food and Drug Administration (FDA) according to the instructions provided by the supplier (Endosafe®-PTS, Charles River Laboratories, Wilmington, MA, USA). These procedures resulted in a sterile final product with endotoxin levels<5 EU/ml. The radiochemical purity was always >97% (mean 97.4±1.5%). The immunoreactive fraction of ^{89}Zr-ibritumomab tiuxetan preparations ranged from 72 to 81% (mean 75.0±3.2%).

Scan protocol

Patients received standard treatment with 250 mg/m^2 Rituxan 1 week before and on the same day prior to both ^{90}Y- and/or ^{89}Zr-ibritumomab tiuxetan administrations. They received approximately 68±11 MBq ^{89}Zr-ibritumomab tiuxetan 31 days before stem cell transplantation (Table 1) followed by three PET scans at 1, 72 and 144 h post-injection (p.i.) covering skull base to femur. Blood samples were drawn at 5, 10, 30 min and 1, 2, 72 and 144 h p.i. for measurement of absolute radioactivity concentrations in whole blood and plasma. In four patients, this was followed 14 days later by 15 MBq/kg or 30 MBq/kg of ^{90}Y-ibritumomab tiuxetan, each in two patients, with a co-injection of 69±6 MBq ^{89}Zr-ibritumomab tiuxetan, again followed by the same PET and blood sampling protocol. The first two patients were treated in hospital; therefore, all urine during the first 72 h after injection was collected and radioactivity in urine was measured. Patients 3 to 7 were treated in our outpatient department, until high-dose chemotherapy started 7 days before stem cell transplantation.

PET scans were made on a dedicated full ring ECAT EXACT HR+ (CTI/Siemens, Knoxville, TN, USA) PET camera in 3-D acquisition mode. Whole-body scans consisted of 7-min emission and 3-min transmission scans per bed position. Data were normalized and corrected for randoms, scatter, attenuation and decay. Attenuation correction was based on a transmission scan with rotating ^{68}Ge rod sources. Images were reconstructed to 128×128 pixels with dimensions 5.15×5.15×2.43 mm using an attenuation- and normalization-weighted ordered subsets expectation maximization (NAW-OSEM) algorithm with 2 iterations with 16 subsets, followed by post-smoothing of the reconstructed image using a 5-mm full-width at half-maximum Gaussian filter. This resulted in images with a spatial resolution of about 7 mm. Quantitative accuracy of ^{89}Zr PET scans was previously confirmed using phantom studies and comparisons between PET-derived and sampled blood radioactivity concentrations, as well as between PET-derived and biopsy tumour radioactivity concentrations [17].

Volume of interest definition

The activity, percentage injected dose (%ID) and standardized uptake value (SUV) normalized to body mass in all organs that could be distinguished from background (lung, liver, spleen and kidneys) were determined using the mean activity concentration in volumes of interest (VOI) drawn over the entire organs using software developed in-house [18]. The activity in tumours was defined by drawing a 50%

Table 1 Patient characteristics

No.	Sex	Age	Weight (kg)	^{89}Zr	^{89}Zr+^{90}Y	^{89}Zr scan 1 (MBq)	^{89}Zr scan 2 (MBq)	^{90}Y (MBq)
1	F	50	84	1, 72, 144	1, 72, 144	49.7	65.5	1,267.7
2	F	50	90	1, 72, 144	1, 72, 144	48.0	88.5	2,473.40
3	M	43	71	1, 72, 144	1, 72, 144	79.2	77.7	1,151.3
4	M	61	78	1, 72, 144	72, 144	74.7	64.8	2,378.8
5	M	46	82	1, 72, 144	–	68.4		
6	M	64	76	72, 144	–	77.5		
7	F	37	82	1, 72	–	75.8		

isocontour VOI. VOIs were drawn separately on all PET scans available for each patient. VOIs were drawn independently over each acquired PET image.

Dosimetry

For calculation of ^{90}Y residence times and absorbed doses, organ and tumour radioactivity were corrected for ^{89}Zr decay, i.e. multiplied by exp(ln(2)t/78.4), with t the time since injection and 78.4 the radioactive half-life of ^{89}Zr in hours, and then uncorrected for decay applying the radioactive half-life of ^{90}Y, i.e. multiplied by exp(−ln(2)t/64.1), with the 64.1 h half-life of ^{90}Y. Residence times for ^{89}Zr- and ^{90}Y-labelled antibodies were calculated as the area under the curve of the organ time-activity data determined by piecewise exponential fitting and assuming only physical decay after the last measurement, divided by the amount of injected activity. Residence time for the red marrow was estimated by assuming a red marrow radioactivity concentration of 30% of the whole blood activity concentration [19]. The residence time of the remainder of the body was calculated as the maximum possible residence time [the radioactive half-life of the tracer divided by ln(2)] minus the sum of residence time of source organs including red marrow, assuming no excretion during the time course of the scans. Tumour absorbed doses were estimated assuming local deposition of all radiation emitted by ^{90}Y. The area under the curve of the tumour time-activity curves was estimated using a single exponential fit to two measured data points at 72 and 144 h p.i. Absorbed doses were calculated using the OLINDA/EXM 1.0 software [20].

Statistical analysis

Total ^{89}Zr-ibritumomab tiuxetan uptake in organs and tumours during the scout procedure and during treatment were compared using regression analysis.

Results

Patient characteristics are shown in Table 1. All patients tolerated ^{89}Zr-ibritumomab tiuxetan well, with no adverse reactions noted. Three patients underwent all scans both prior to and during therapy. Two patients (1 and 3) received standard therapy activity of ^{90}Y-ibritumomab tiuxetan and two patients (2 and 4) were treated with a higher ^{90}Y-ibritumomab tiuxetan activity. Three patients (5–7) did not receive the co-injection of ^{89}Zr- and ^{90}Y-ibritumomab tiuxetan because of logistical problems. One patient (7) had to be excluded from further analysis because he did not undergo a third PET scan (144 h p.i.) because of scanner problems. In total, data from six patients could be used to assess biodistribution of ^{89}Zr-ibritumomab tiuxetan at 72 and 144 h p.i. Calculation of residence times in the first three patients, both with and without the 1-h p.i. scans, revealed no significant differences due to exclusion of the first scan (Pearson correlation coefficient r=0.99, linear regression with and without 1-h p.i. data point). Therefore, dosimetry data of patients 4 and 6 were included in the analysis and data from four patients could be used to compare biodistribution of ^{89}Zr-ibritumomab tiuxetan prior to and during therapy.

Images at 1 h p.i. showed mainly blood pool activity and activity in heart, liver, spleen, bone marrow and kidneys. No activity was seen at tumour sites. The images at 72 and 144 h p.i. showed increasing activity on tumour sites and decreasing activity in source organs (Fig. 1). Negligible amounts of activity (<1% of administered activity) were found in urine.

Figure 2 shows SUV as a function of time for all source organs. As shown in Fig. 3, a strong correlation between estimated absorbed doses in different organs with ^{89}Zr-ibritumomab tiuxetan without ^{90}Y-ibritumomab tiuxetan and ^{89}Zr-ibritumomab tiuxetan with ^{90}Y-ibritumomab tiuxetan was found (r=0.97). The highest mean ^{90}Y absorbed dose as calculated from the ^{89}Zr-ibritumomab tiuxetan biodistribution was seen in the liver with 3.2±1.8 mGy/MBq (range 1.8–6.6 mGy/MBq, Table 2). However, absorbed dose to the spleen (2.9±0.7 mGy/MBq, range 1.8–3.8 mGy/MBq) was,

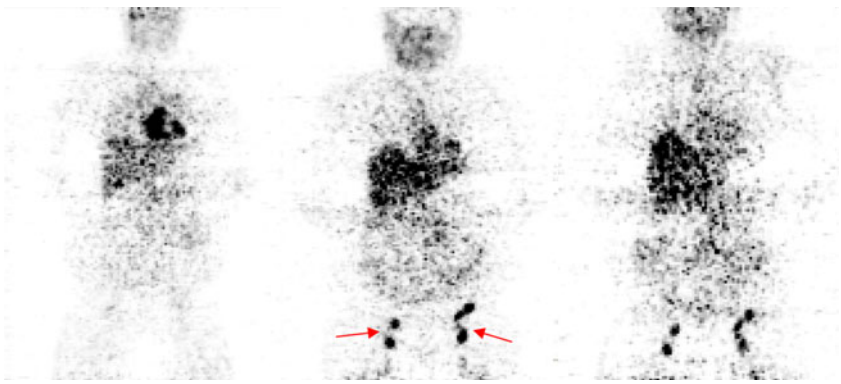

Fig. 1 Typical coronal section ^{89}Zr-ibritumomab tiuxetan images at 1, 72 and 144 h p.i. *Arrows* indicate tumour localizations

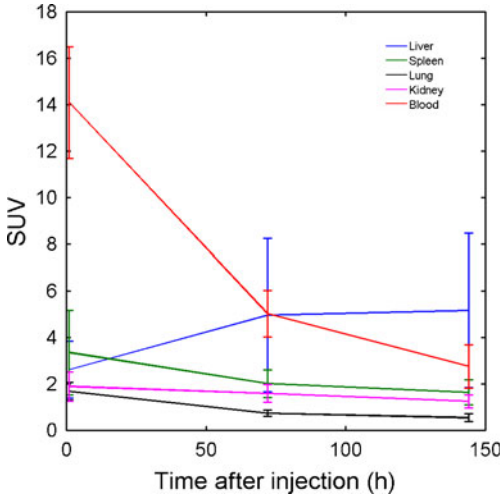

Fig. 2 ^{89}Zr-ibritumomab tiuxetan SUV versus time after injection in liver, spleen, lung, kidneys and blood (mean ± SD, n=6)

although marginally, higher in five of six patients. The effective dose was 0.87±0.14 mSv/MBq. Table 3 shows effective half-lives of ^{90}Y-ibritumomab tiuxetan for the 1–72 and 72–144 h intervals. As expected, no effect of the higher treatment activity of ^{90}Y-ibritumomab tiuxetan on the biodistribution in two of the four patients was seen, although this could not be tested statistically due to the small patient groups.

Tumour absorbed dose estimates were made for the 4 patients that underwent ^{89}Zr-ibritumomab tiuxetan scans both prior to and during therapy with ^{90}Y-ibritumomab tiuxetan, with 13 tumour localizations in total. The average size of the lesion VOIs was 3.3 cm^3 (range 0.8–11.3 cm^3). Tumour absorbed doses ranged from 8.6 to 28.6 mGy/MBq (mean 14.9 mGy/MBq). Figure 4 shows estimated tumour

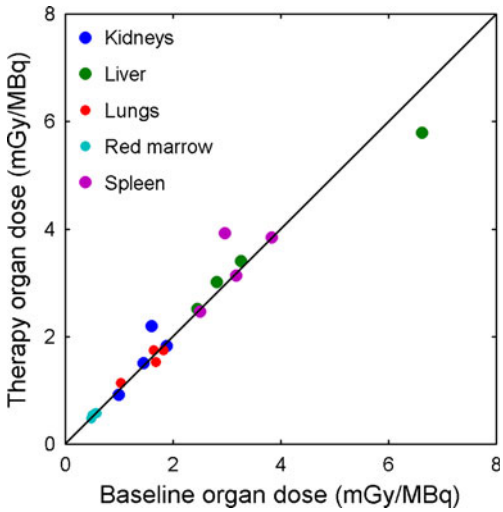

Fig. 3 Absorbed organ doses estimated using a scout scan with ^{89}Zr-ibritumomab tiuxetan prior to therapy versus those estimated using a simultaneous administration of ^{89}Zr-ibritumomab tiuxetan and ^{90}Y-ibritumomab tiuxetan. The *solid line* is the line of identity

absorbed doses. Correlation between absorbed doses estimated using a scout scan and during therapy was moderate (r=0.75), with no significant differences between baseline and therapy absorbed dose estimates (p=0.09, two-tailed paired t test).

Figure 5 shows the correlation between SUV of ^{89}Zr-ibritumomab tiuxetan and absorbed dose of ^{90}Y-ibritumomab tiuxetan in the liver. Correlation was high for SUV at 72 h p.i. as well as 144 h p.i. (both r=0.99), with a nearly identical relationship between SUV and absorbed dose for both time points (slope 0.50 and 0.49 mGy·MBq^{-1}·SUV^{-1}; intercept 0.85 and 0.89 mGy/MBq, respectively).

Discussion

To our knowledge, this is the first study describing the biodistribution and radiation dosimetry of ^{90}Y-ibritumomab tiuxetan therapy as assessed by ^{89}Zr-ibritumomab tiuxetan PET. All prior studies aiming to estimate ^{90}Y-ibritumomab tiuxetan absorbed doses were performed using ^{111}In-ibritumomab tiuxetan and single photon imaging. The advantage of using a positron-emitting isotope is that PET is inherently quantitative, whereas quantification with, especially planar, gamma camera imaging involves considerable uncertainties that can often surpass estimated activity concentrations themselves. Comparison of measured trues and random count rates as measured during scout scans and during scans with both ^{89}Zr and therapeutic amounts of ^{90}Y showed that the presence of ^{90}Y had no effect on PET count rates and hence did not influence quantitative accuracy.

Although the results of the present work are generally consistent with previous studies using ^{111}In-ibritumomab tiuxetan, there are a few important differences. The highest absorbed dose in the current work was found for the liver (3.2±1.8 mGy/MBq, range 1.5–6.6 mGy/MBq) and the spleen (2.9±0.7 mGy/MBq, range 1.8–3.6 mGy/MBq). Wiseman et al. [13], using ^{111}In-ibritumomab tiuxetan in a study population of follicular lymphomas and transformed B-cell NHL, found the highest absorbed dose in the spleen with a median absorbed dose of 7.30 mGy/MBq with a range of 3.50–26.0 mGy/MBq followed by liver (4.60, range 2.20–11.0 mGy/MBq), lungs (1.90 mGy/MBq, range 1.30–4.30 mGy/MBq), red marrow (0.65 mGy/MBq, range 0.26–1.10 mGy/MBq) and kidneys (0.20 mGy/MBq, range (0.01–0.65 mGy/MBq). Although Fisher et al. [14], with a study population of low- and intermediate-grade NHL, found an absorbed dose to the spleen of 4.7±2.3 mGy/MBq, closer to the results in the current study, the spleen was the organ with the highest absorbed dose, followed by liver (3.6±1.4 mGy/MBq), red marrow (2.7±0.9 mGy/MBq), kidneys (2.4±0.6 mGy/MBq) and lungs (0.8±0.8 mGy/MBq). Shen et al. [21], using ^{111}In-ibritumomab

Table 2 ^{89}Zr-ibritumomab tiuxetan and ^{90}Y-ibritumomab tiuxetan organ residence times and absorbed doses as estimated using a scout scan with ^{89}Zr-ibritumomab tiuxetan (n=6)

	^{89}Zr-ibritumomab tiuxetan		^{90}Y-ibritumomab tiuxetan	
	Residence time Mean ± SD (h)	Absorbed dose Mean ± SD (mGy/MBq)	Residence time Mean ± SD (h)	Absorbed dose Mean ± SD (range) (mGy/MBq)
Liver	11.6±4.8	1.36±0.58	9.9±4.1	3.2±1.8 (1.5–6.6)
Spleen	1.08±0.31	1.04±0.16	0.95±0.26	2.88±0.67 (1.83–3.83)
Kidney	0.93±0.22	0.754±0.062	0.81±0.19	1.46±0.31 (0.99–1.88)
Lung	2.83±0.55	0.63±0.11	2.54±0.48	1.47±0.34 (1.07–1.82)
Red marrow	0.59±0.22	0.460±0.047	0.48±0.10	0.520±0.041 (0.485–0.581)
Remainder[a]	96±5		78±4	
Effective dose (mSv/MBq)		0.55±0.07		0.87±0.14

[a] Based on maximum residence time minus sum of source organ residence times

tiuxetan as well, also found the spleen to be the organ receiving the highest absorbed dose with a median absorbed dose of 6.1 mGy/MBq (range 1.8–17.8 mGy/MBq). Absorbed dose estimates from all publications referred to above and from the Zevalin package insert are summarized in Table 4. The doses from the Zevalin package insert were estimated with ^{111}In-Zevalin. In this study, the spleen is the organ with the highest absorbed dose as well, at 9.4 mGy/MBq (range 1.8–20.0 mGy/MBq). Shen et al. (study population of follicular or transformed CD20-positive B-cell NHL) administered ^{111}In-ibritumomab tiuxetan with and without additional treatment with rituximab and found no difference in absorbed radiation dose before and during treatment except in the spleen where a significant decrease of residence time was found. They also analysed the tumour absorbed dose which was consistent with our data with a median absorbed dose of 18.1 mGy/MBq (range 4.7–98.9 mGy/MBq). Shen et al. showed a decrease in residence time and volume of the spleen after long-term rituximab treatment compared to a single dose of rituximab before ^{111}In/^{90}Y-ibritumomab tiuxetan. This could also apply to our study population and explain the difference from the four other studies where a single dose of rituximab was given prior to ibritumomab tiuxetan therapy. This observation is also in agreement with the study of Illidge et al. [22].

Table 3 Mean (± SD) effective half-life of ^{90}Y-ibritumomab tiuxetan as estimated using a scout scan with ^{89}Zr-ibritumomab tiuxetan (1–72 h: n=5; 72–144 h: n=6)

	Effective half-life (h)	
	1–72 h p.i.	72–144 h p.i.
Liver	185±124	74±8
Spleen	43±15	54±6
Kidney	57±22	51±15
Lung	32±6	42±9
Blood	42±9	66±20

Differences in biodistribution between ^{111}In-mAb and ^{90}Y-mAb conjugates have been observed before in vivo in tumour-bearing mice and in cancer patients [23–25]. Perk et al. [26] showed in their study that biodistribution of ^{89}Zr-Df-cetuximab and ^{88}Y-DOTA-cetuximab (^{88}Y as a substitute for ^{90}Y) is comparable for all observed organs, except differences in bone accumulation (sternum and thigh bone). What is more, the same was shown for ^{89}Zr-ibritumomab tiuxetan and ^{90}Y-ibritumomab tiuxetan in NHL-bearing mice [15]. Therefore, we can state that ^{89}Zr-ibritumomab tiuxetan absorbed doses in liver and spleen are representative for ^{90}Y-ibritumomab tiuxetan. Furthermore, the discrepancy between ^{111}In-ibritumomab tiuxetan and ^{89}Zr-ibritumomab tiuxetan uptake in liver and especially spleen has been described before when comparing ^{111}In-DTPA-octreotide and ^{86}Y-DOTA-octreotide as

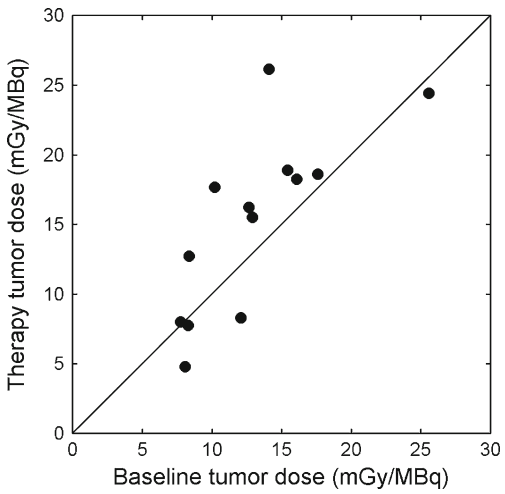

Fig. 4 Absorbed tumour doses estimated using a scout scan with ^{89}Zr-ibritumomab tiuxetan prior to therapy versus those estimated using a simultaneous administration of ^{89}Zr-ibritumomab tiuxetan and ^{90}Y-ibritumomab tiuxetan. The *solid line* is the line of identity

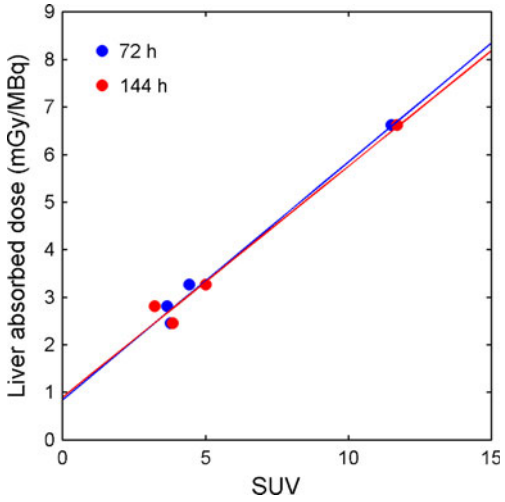

Fig. 5 Absorbed ^{90}Y dose to the liver, based on scout scans with ^{89}Zr-ibritumomab tiuxetan, versus SUV of ^{89}Zr-ibritumomab tiuxetan at 72 and 144 h p.i. The *solid lines* represent linear fits to the data

analogues of ^{90}Y-DOTA-octreotide [27]. In this study ^{111}In-DTPA-octreotide was shown to overestimate absorbed dose in kidneys and spleen, whereas absorbed dose to liver was underestimated in comparison to ^{86}Y-DOTA-octreotide.

The effective dose found in the present study was generally higher than found in previous studies using ^{111}In-ibritumomab tiuxetan (0.87±0.14 mSv/MBq compared to~ 0.5 mSv/MBq). The remainder of the body residence times were based on the assumption of no excretion of radioactivity, which is likely to lead to conservative effective dose estimates in the current study. Using whole-body VOIs instead, which in the present work would not include the legs, would have resulted in somewhat lower effective doses (mean 0.72 mSv/MBq). However, because the energy of the radiation emitted by ^{90}Y is deposited within the same organ only, this does not affect ^{90}Y-ibritumomab tiuxetan organ absorbed doses.

Red marrow and liver absorbed doses were 26 and 9% of the threshold for nonstochastic effects (2 and 35 Gy, respectively) [28]. Since the liver is the dose-limiting organ in patients undergoing auSCT, this implies that a considerably higher amount than 30 MBq/kg can be given to these patients without resulting in deterministic effects. Clinically, no significant abnormalities were seen and no significant decreases of liver function or liver function abnormalities were seen in this particular group of patients. Use of blood data to estimate marrow absorbed doses may underestimate dosimetry results if there is any interaction of the targeting agent with the bone marrow. However, this is not relevant for the patient group discussed in the present work, since patients will undergo auSCT following therapy.

Relative to organ dosimetry, tumour dosimetry shows a moderate correlation between baseline and therapy scans. This is most probably due to the small volumes of the tumours comparing the organ volumes, resulting in increased uncertainty in measurement of radioactivity concentrations. Tumour VOIs were drawn as 50% isocontours independently on each image, as recommended in the European Association of Nuclear Medicine procedure guidelines for tumour imaging with ^{18}F-FDG [29]. The size of these isocontour VOIs is dependent on the statistically uncertain values for the maximum pixel, and variations in tumour VOI sizes over time result in variations in partial volume errors, which further affect the accuracy of absorbed dose estimates. To minimize these effects, tumour VOIs could be based on anatomical information (e.g. coregistered CT or MRI scans, preferably acquired using PET/CT or PET/MRI scanners), and partial volume corrections could be applied based on the anatomical information. Since the data in the present study were acquired on a stand-alone PET scanner, VOIs could not be drawn on coregistered CT images and no attempts to further improve the quantitative accuracy of tumour measurements were made. In addition, the limited number of data points and resulting uncertainty in tumour uptake, especially during the first 24–48 h after injection, may contribute to the low tumour dose correlation.

As Fig. 5 shows, SUV of ^{89}Zr-ibritumomab tiuxetan at either 72 or 144 h p.i. may be a good predictor of the absorbed radiation dose to the liver during ^{90}Y-ibritumomab tiuxetan therapy, although this should be confirmed in a larger study. Therefore, a single PET scan of the liver at 3 or 6 days after injection of ^{89}Zr-ibritumomab tiuxetan could be sufficient to estimate the maximum amount of ^{90}Y-ibritumomab tiuxetan that can be administered to an individual patient who will also undergo auSCT. This strategy will lead

Table 4 Comparison of median absorbed doses of ^{90}Y-ibritumomab tiuxetan for selected organs in mGy/MBq in different studies

	Liver	Spleen	Kidney	Lung	Red marrow	Whole body (mSv/MBq)
Current study	3.2 (1.5–6.6)	2.9 (1.8–3.6)	1.46 (0.99–1.88)	1.47 (1.07–1.82)	0.52 (0.49–0.58)	0.87 (0.70–1.06)
Wiseman et al. [13]	4.60 (2.20–11.0)	7.30 (3.50–26.0)	0.20 (<0.01–0.65)	1.90 (1.30–4.30)	0.65 (0.26–1.10)	0.54 (0.46–0.78)
Fisher et al. [14]	3.1 (2.3–6.6)	4.3 (0.98–9.0)	2.4 (1.4–3.9)	0.60 (0.31–1.6)	2.4 (1.7–4.5)	0.55 (0.44–0.81)
Shen et al. [21]	3.66 (2.11–11.62)	6.14 (1.82–17.76)	3.31 (1.95–4.65)	1.10 (0.41–2.31)	0.79 (0.32–1.22)	0.48 (0.24–0.86)
^{90}Y-Zevalin®	4.8 (2.9–8.1)	9.4 (1.8–20.0)	0.1 (0.0–0.3)	2.0 (1.2–3.4)	1.3 (0.6–1.8)	0.5 (0.4–.07)

to a therapy increasingly tailored to the individual patient. Although the present protocol requires administration of Rituxan prior to the pretreatment scan as well, this has limited influence on clinical feasibility since this is part of the routine treatment of the present patient group. Poor uptake in the tumour at the pre-therapy scan cannot be a reason to exclude patients from receiving this therapy. In tumour, not only the effect of RIT is important, but also the effect of Rituxan. Additional studies are needed for improved assessment of tumour dosimetry.

Conclusion

Biodistribution of ^{89}Zr-ibritumomab tiuxetan is not influenced by simultaneous therapy with ^{90}Y-ibritumomab tiuxetan. Therefore, a pre-therapy scan with ^{89}Zr-ibritumomab tiuxetan can be used to accurately predict radiation dosimetry during treatment with ^{90}Y-ibritumomab tiuxetan. Absorbed doses to the spleen were lower than those previously estimated using ^{111}In-ibritumomab tiuxetan. The dose-limiting organ in patients undergoing stem cell transplantation is the liver. In the future, a single ^{89}Zr-ibritumomab tiuxetan PET scan may be sufficient to optimize the administered amount of ^{90}Y-ibritumomab tiuxetan RIT in the individual patient when combined with auSCT.

Acknowledgement The authors thank the staff at the Department of Nuclear Medicine & PET Research for their assistance in performing the PET scans.

Conflicts of interest None.

References

1. Parkin DM, Bray F, Ferlay J, Pisani P. Global cancer statistics, 2002. CA Cancer J Clin 2005;55:74–108.
2. Palanca-Wessels MC, Press OW. Improving the efficacy of radioimmunotherapy for non-Hodgkin lymphomas. Cancer 2010;116(4 Suppl):1126–33.
3. Gopal AK, Gooley TA, Golden JB, Maloney DG, Bensinger WI, Petersdorf SH, et al. Efficacy of high-dose therapy and autologous hematopoietic stem cell transplantation for non-Hodgkin's lymphoma in adults 60 years of age and older. Bone Marrow Transplant 2001;27:593–9.
4. Marcus R, Imrie K, Belch A, Cunningham D, Flores E, Catalano J, et al. CVP chemotherapy plus rituximab compared with CVP as first-line treatment for advanced follicular lymphoma. Blood 2005;105:1417–23.
5. Hiddemann W, Kneba M, Dreyling M, Schmitz N, Lengfelder E, Schmits R, et al. Frontline therapy with rituximab added to the combination of cyclophosphamide, doxorubicin, vincristine, and prednisone (CHOP) significantly improves the outcome for patients with advanced-stage follicular lymphoma compared with therapy with CHOP alone: results of a prospective randomized study of the German Low-Grade Lymphoma Study Group. Blood 2005;106:3725–32.
6. Herold M, Dölken G, Fiedler F, Franke A, Freund M, Helbig W, et al. Randomized phase III study for the treatment of advanced indolent non-Hodgkin's lymphomas (NHL) and mantle cell lymphoma: chemotherapy versus chemotherapy plus rituximab. Ann Hematol 2003;82:77–9.
7. Kaminski MS, Tuck M, Estes J, Kolstad A, Ross CW, Zasadny K, et al. 131I-tositumomab therapy as initial treatment for follicular lymphoma. N Engl J Med 2005;352:441–9.
8. Winter JN. Combining yttrium 90-labeled ibritumomab tiuxetan with high-dose chemotherapy and stem cell support in patients with relapsed non-Hodgkin's lymphoma. Clin Lymphoma 2004;5 Suppl 1:S22–6.
9. Nademanee A, Forman S, Molina A, Fung H, Smith D, Dagis A, et al. A phase 1/2 trial of high-dose yttrium-90-ibritumomab tiuxetan in combination with high-dose etoposide and cyclophosphamide followed by autologous stem cell transplantation in patients with poor-risk or relapsed non-Hodgkin lymphoma. Blood 2005;106:2896–902.
10. Witzig TE, Gordon LI, Cabanillas F, Czuczman MS, Emmanouilides C, Joyce R, et al. Randomized controlled trial of yttrium-90-labeled ibritumomab tiuxetan radioimmunotherapy versus rituximab immunotherapy for patients with relapsed or refractory low-grade, follicular, or transformed B-cell non-Hodgkin's lymphoma. J Clin Oncol 2002;20:2453–63.
11. Devizzi L, Guidetti A, Tarella C, Magni M, Matteucci P, Seregni E, et al. High-dose yttrium-90-ibritumomab tiuxetan with tandem stem-cell reinfusion: an outpatient preparative regimen for autologous hematopoietic cell transplantation. J Clin Oncol 2008;26:5175–82.
12. Ferrucci PF, Vanazzi A, Grana CM, Cremonesi M, Bartolomei M, Chinol M, et al. High activity 90Y-ibritumomab tiuxetan (Zevalin) with peripheral blood progenitor cells support in patients with refractory/resistant B-cell non-Hodgkin lymphomas. Br J Haematol 2007;139:590–9.
13. Wiseman GA, Leigh B, Erwin WD, Lamonica D, Kornmehl E, Spies SM, et al. Radiation dosimetry results for Zevalin radioimmunotherapy of rituximab-refractory non-Hodgkin lymphoma. Cancer 2002;94(4 Suppl):1349–57.
14. Fisher DR, Shen S, Meredith RF. MIRD dose estimate report No. 20: radiation absorbed-dose estimates for 111In- and 90Y-ibritumomab tiuxetan. J Nucl Med 2009;50:644–52.
15. Perk LR, Visser OJ, Stigter-van Walsum M, Vosjan MJ, Visser GW, Zijlstra JM, et al. Preparation and evaluation of (89)Zr-Zevalin for monitoring of (90)Y-Zevalin biodistribution with positron emission tomography. Eur J Nucl Med Mol Imaging 2006;33:1337–45.
16. Verel I, Visser GW, Boellaard R, Stigter-van Walsum M, Snow GB, van Dongen GA. 89Zr immuno-PET: comprehensive procedures for the production of 89Zr-labeled monoclonal antibodies. J Nucl Med 2003;44:1271–81.
17. Börjesson PK, Jauw YW, de Bree R, Roos JC, Castelijns JA, Leemans CR, et al. Radiation dosimetry of 89Zr-labeled chimeric monoclonal antibody U36 as used for immuno-PET in head and neck cancer patients. J Nucl Med 2009;50:1828–36.
18. Boellaard R, Hoekstra OS, Lammertsma AA. Software tools for standardized analysis of FDG whole body studies in multi-center trials [abstract]. J Nucl Med 2008;49 (Suppl 1):159P.
19. Wessels BW, Bolch WE, Bouchet LG, Breitz HB, Denardo GL, Meredith RF, et al. Bone marrow dosimetry using blood-based models for radiolabeled antibody therapy: a multiinstitutional comparison. J Nucl Med 2004;45:1725–33.
20. Stabin MG, Sparks RB, Crowe E. OLINDA/EXM: the second-generation personal computer software for internal dose assessment in nuclear medicine. J Nucl Med 2005;46:1023–7.

21. Shen S, Forero A, Meredith RF, Shah JJ, Knox SJ, Wiseman GA, et al. Impact of rituximab treatment on (90)Y- ibritumomab dosimetry for patients with non-Hodgkin lymphoma. J Nucl Med 2010;51:150–7.
22. Illidge TM, Bayne M, Brown NS, Chilton S, Cragg MS, Glennie MJ, et al. Phase 1/2 study of fractionated (131)I-rituximab in low-grade B-cell lymphoma: the effect of prior rituximab dosing and tumor burden on subsequent radioimmunotherapy. Blood 2009;113:1412–21.
23. Carrasquillo JA, White JD, Paik CH, Raubitschek A, Le N, Rotman M, et al. Similarities and differences in 111In- and 90Y-labeled 1B4M-DTPA antiTac monoclonal antibody distribution. J Nucl Med 1999;40:268–76.
24. Camera L, Kinuya S, Garmestani K, Brechbiel MW, Wu C, Pai LH, et al. Comparative biodistribution of indium- and yttrium-labeled B3 monoclonal antibody conjugated to either 2-(p-SCN-Bz)-6-methyl-DTPA (1B4M-DTPA) or 2-(p-SCN-Bz)-1,4,7,10-tetraazacyclododecane tetraacetic acid (2B-DOTA). Eur J Nucl Med 1994;21:640–6.
25. Garmestani K, Milenic DE, Plascjak PS, Brechbiel MW. A new and convenient method for purification of 86Y using a Sr(II) selective resin and comparison of biodistribution of 86Y and 111In labelled Herceptin. Nucl Med Biol 2002;29:599–606.
26. Perk LR, Visser GW, Vosjan MJ, Stigter-van Walsum M, Tijink BM, Leemans CR, et al. (89)Zr as a PET surrogate radioisotope for scouting biodistribution of the therapeutic radiometals (90)Y and (177)Lu in tumor-bearing nude mice after coupling to the internalizing antibody cetuximab. J Nucl Med 2005;46:1898–906.
27. Helisch A, Förster GJ, Reber H, Buchholz HG, Arnold R, Göke B, et al. Pre-therapeutic dosimetry and biodistribution of 86Y-DOTA-Phe1-Tyr3-octreotide versus 111In-pentetreotide in patients with advanced neuroendocrine tumours. Eur J Nucl Med Mol Imaging 2004;31:1386–92.
28. ICRP-41. Nonstochastic effects of ionizing radiation. Ann ICRP 1984;14:1–33.
29. Boellaard R, O'Doherty MJ, Weber WA, Mottaghy FM, Lonsdale MN, Stroobants SG, et al. FDG PET and PET/CT: EANM procedures guidelines for tumour PET imaging: version 1.0. Eur J Nucl Med Mol Imaging 2010;37:181–200.